

AIDIC



Associazione
Termotecnica
Italiana

Cicli webinar "fil rouge" 2021

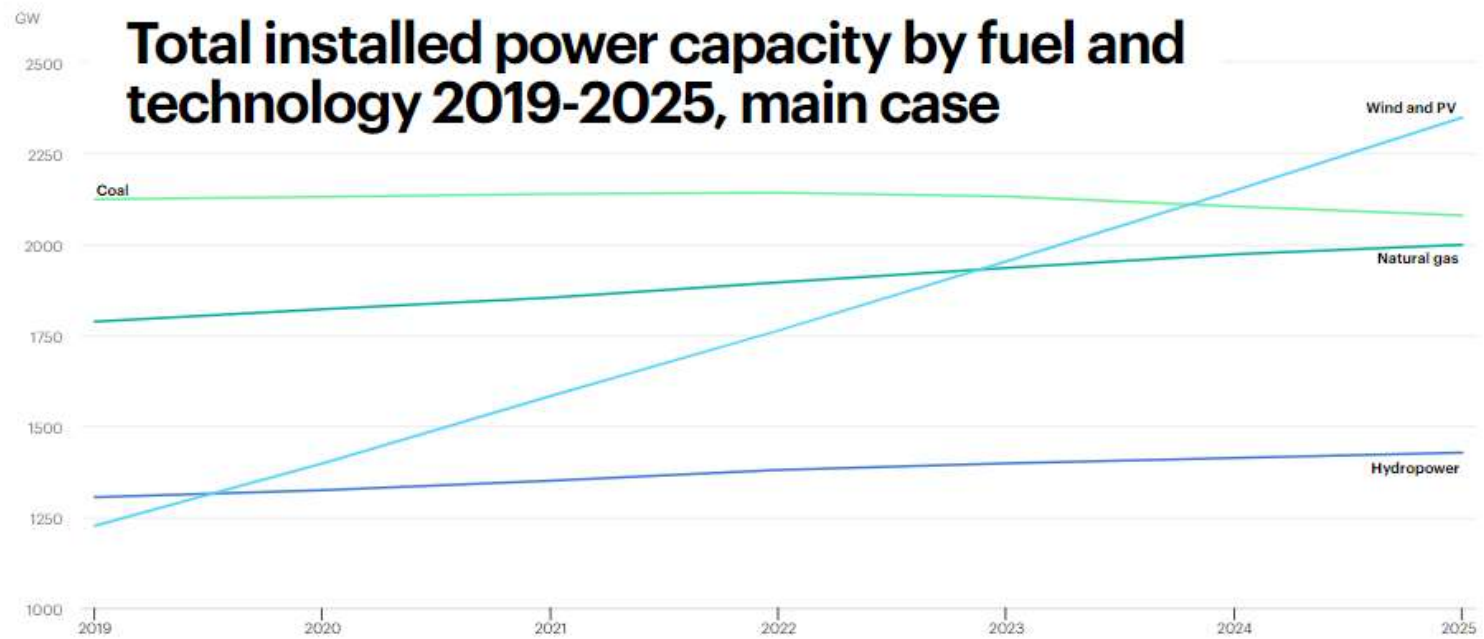
LA TRANSIZIONE ENERGETICA
3 GIUGNO

Prospettive dell'Elettrocatalisi nell'Industria Chimica

Martino Di Serio

NICL, Dipartimento di Scienze Chimiche – Università di Napoli Federico II

NICL
Naples Industrial Chemistry Laboratory
www.nicl.it



IEA, Total installed power capacity by fuel and technology 2019-2025, main case, IEA, Paris <https://www.iea.org/data-and-statistics/charts/total-installed-power-capacity-by-fuel-and-technology-2019-2025-main-case>

PRODUZIONE LORDA DI ENERGIA ELETTRICA ITALIA

GWh; anni 1997-2019

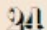
	2018	2019*	Variazione (2018-2019)
Solidi	28'470	15'111	-46.92%
Gas naturale	128'538	143'198	11.41%
Prodotti petroliferi	3'289	3'369	2.43%
Altri	13'281	13'454	1.30%
Totale termoelettrico (A)	173'578	175'132	0.90%
Idroelettrico da pompaggi (B)	1'716	1'723	0.41%
Idroelettrico (da apporti naturali)	48'786	45'776	-6.17%
Eolico	17'716	20'245	14.28%
Fotovoltaico	22'654	23'689	4.57%
Geotermico	6'105	6'031	-1.21%
Biomassa e rifiuti	19'153	19'097	-0.29%
Totale rinnovabili (C)	114'414	114'838	0.37%
Totale (A+B+C)	289'708	291'693	0.69%

La voce "Prodotti petroliferi" comprende: olio combustibile, orimulsion, distillati leggeri, gasolio, coke di petrolio, bassi prodotti e altri residui della lavorazione del petrolio.

La voce "Altri" comprende: gas derivati, recuperi di calore ed espansione del gas compresso.

* Dati provvisori

Fonte: Elaborazioni Arera su dati GRTN/TERNA.

 **Economia** Energia e ambiente

Transizione energetica

Rinnovabili flop. Deserta la gara Gse, assegnato solo il 12% degli incentivi

Il ministro Cingolani annuncia un nuovo decreto entro l'estate. Contratti diretti di fornitura di elettricità verde Axpo, Canadian, Solvay, Falck

di J.G.

27 maggio 2021

Il drammatico quinto bando

Di mese in mese, le aste per assegnare gli incentivi alle rinnovabili sono sempre più deserte. Il risultato del quinto bando ha visto svaporare l'88% delle offerte per incentivi alle rinnovabili, mentre il bando precedente aveva allocato un già modesto 25% di offerte di incentivi a solare, eolico e altre tecnologie rinnovabili.

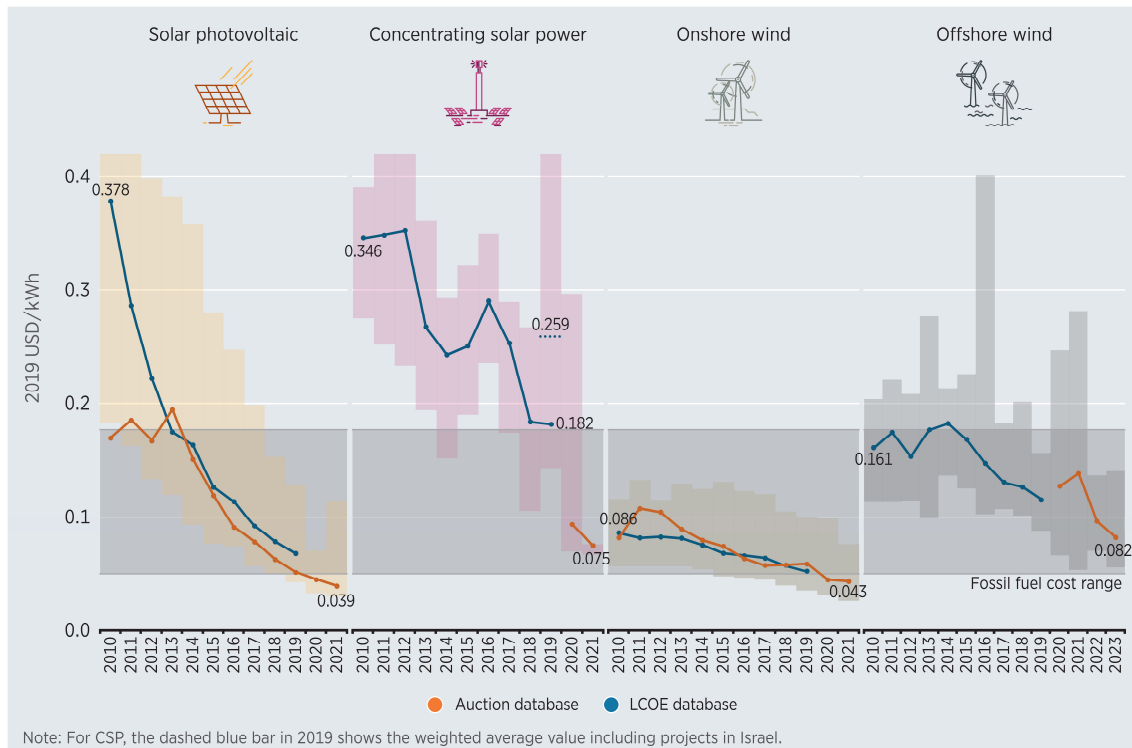
Corrono i contratti diretti: Axpo, Canadian, Solvay, Falck

Anche il colosso chimico belga Solvay punta sull'energia rinnovabile e ha firmato un corporate power purchase agreement (Ppa) fisico con Falck Renewables della durata di 10 anni per lo sviluppo di un progetto solare in Puglia. Il 70% dell'elettricità prodotta dall'impianto solare andrà a beneficio di quattro dei sei stabilimenti italiani di Solvay: Bollate, Ospiate, Livorno e Rosignano, ottenendo una riduzione di emissioni annue di CO2 di oltre 15mila tonnellate.

Corrono

RENEWABLE POWER GENERATION INCREASINGLY OUT-COMPETES FOSSIL FUELS

Global weighted average LCOE and Auction/PPA prices for CSP, onshore and offshore wind, and solar PV, 2010 to 2023



The thick lines are the global weighted average *LCOE, or auction values, by year. The grey bands that vary by year are cost/price range for the 5th and 95th percentiles of projects.. For the LCOE data, the real WACC** is 7.5% for OECD countries and China, and 10% for the rest of the world. The band that crosses the entire chart represents the fossil fuel-fired power generation cost range.

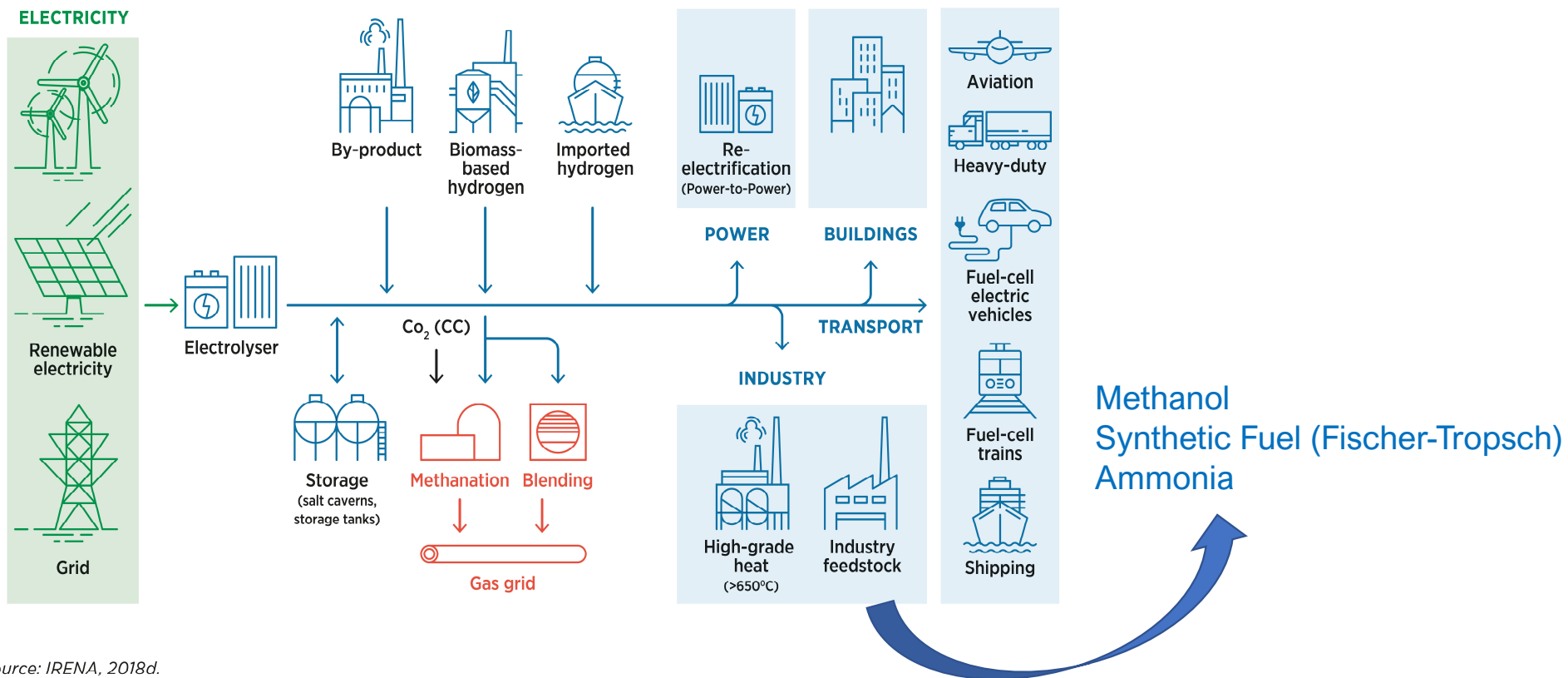
RENEWABLE POWER GENERATION COSTS 2019, International Renewable Energy Agency (IRENA)

*Global Data on Levelized Cost Of Electricity Generation (LCOE)
 **Weighted average cost of capital (WACC)

***Innovation landscape for a renewable-powered future:**

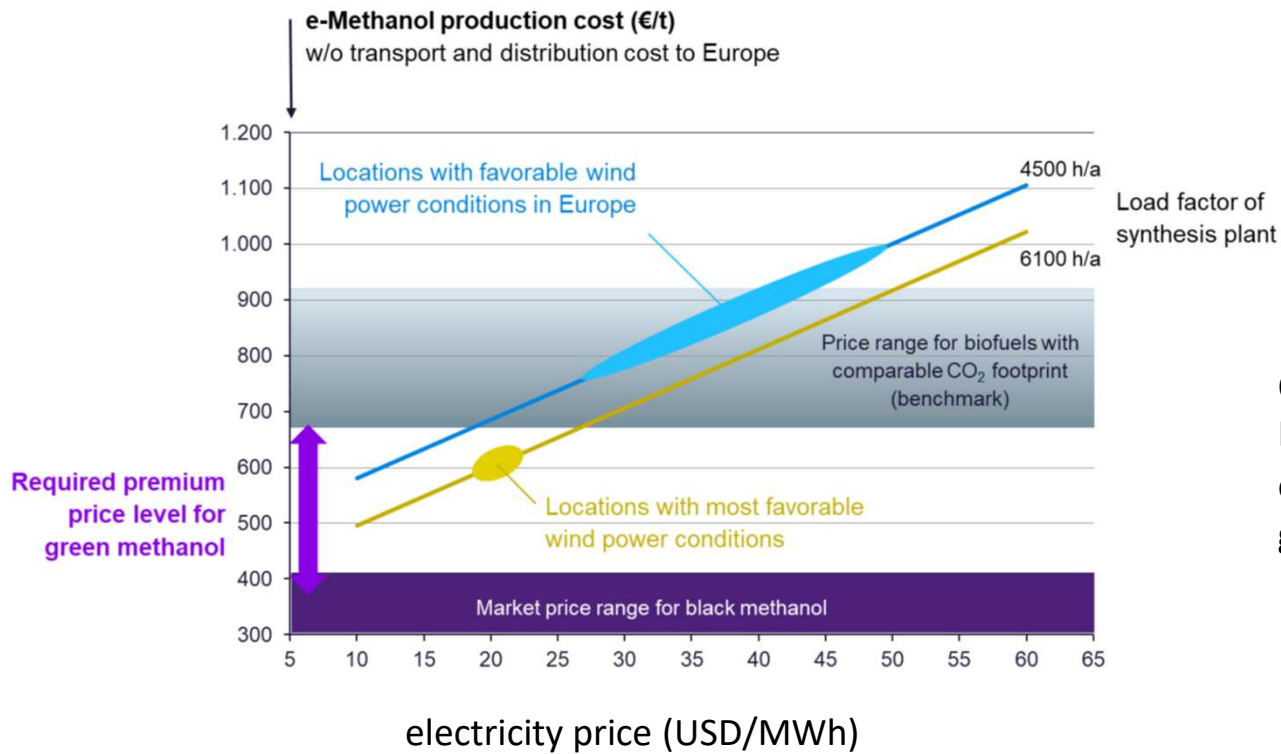
Solution XI: Power to X

Integration of variable renewable energy (VRE) into end-uses by means of hydrogen



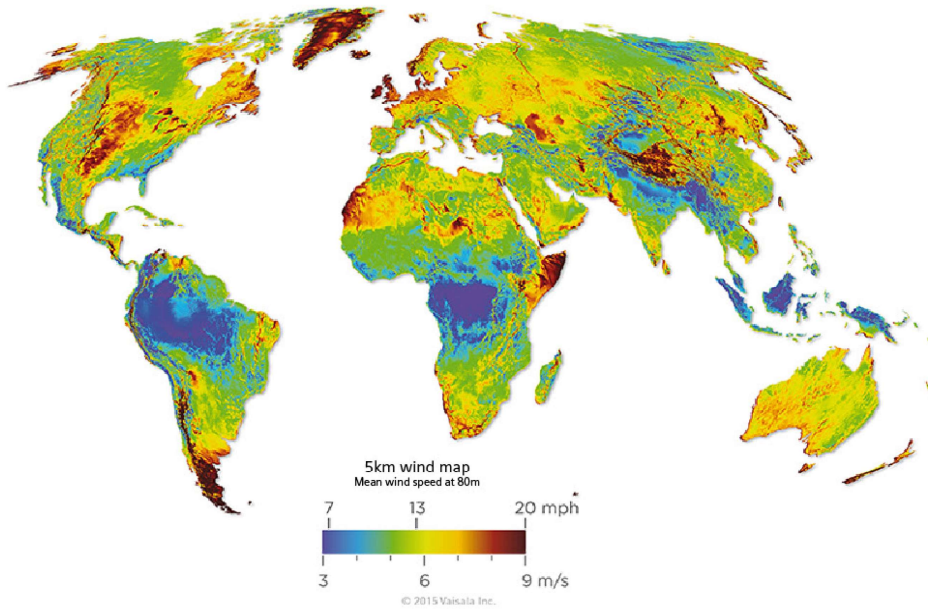
Source: IRENA, 2018d.

[*https://www.irena.org/publications/2019/Feb/Innovation-landscape-for-a-renewable-powered-future](https://www.irena.org/publications/2019/Feb/Innovation-landscape-for-a-renewable-powered-future)

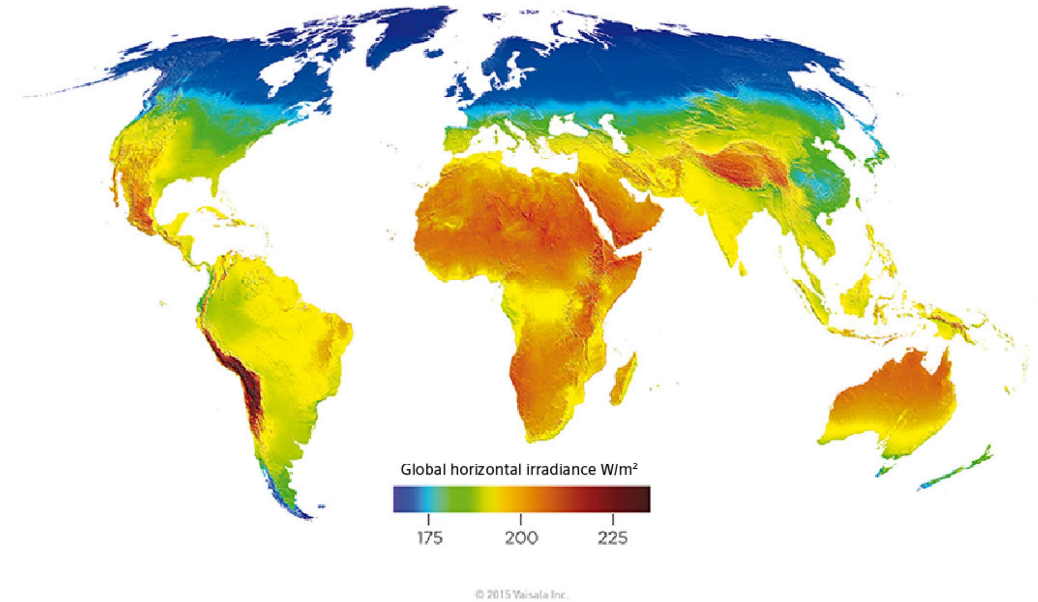


Only one small commercial plant (4 kt/yr) in Iceland uses green Hydrogen from water electrolysis and CO₂ taken from local geological sources.

There are many regions worldwide benefiting from the generation of power from renewable sources



Global wind map

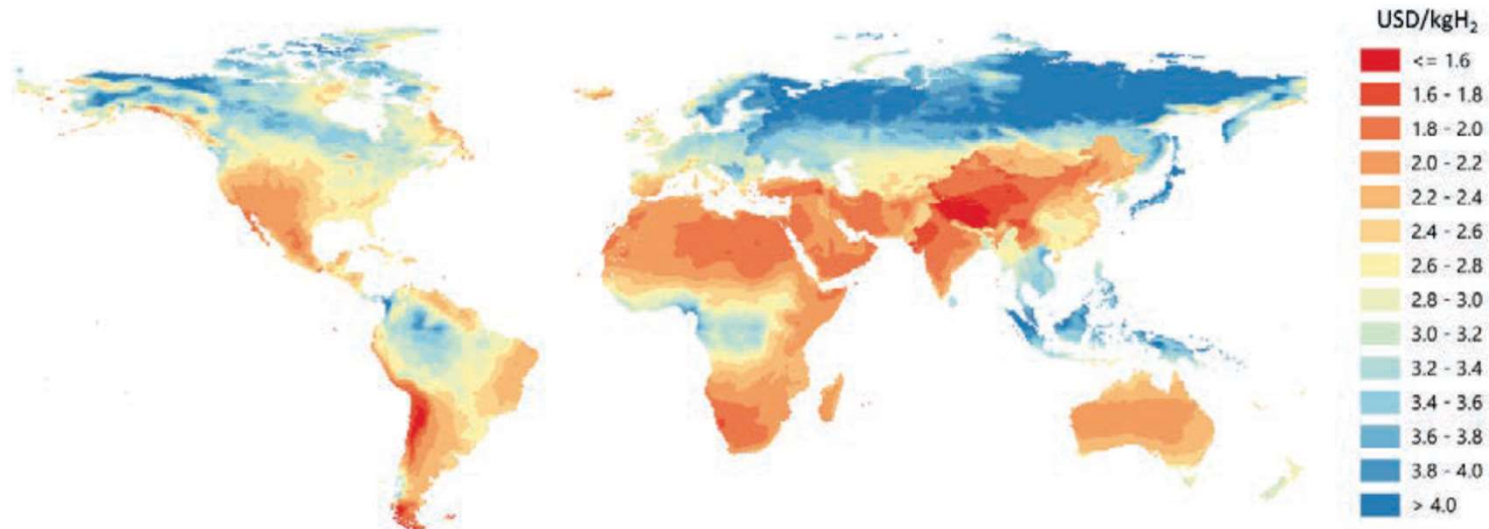


Global solar map

Graphics from Tanja Siegel – independent-medien-design.de

White paper | Power-to-X: A closer look at e-Ammonia. Siemens 2021

Hydrogen costs from hybrid solar PV and onshore wind systems in the long term.

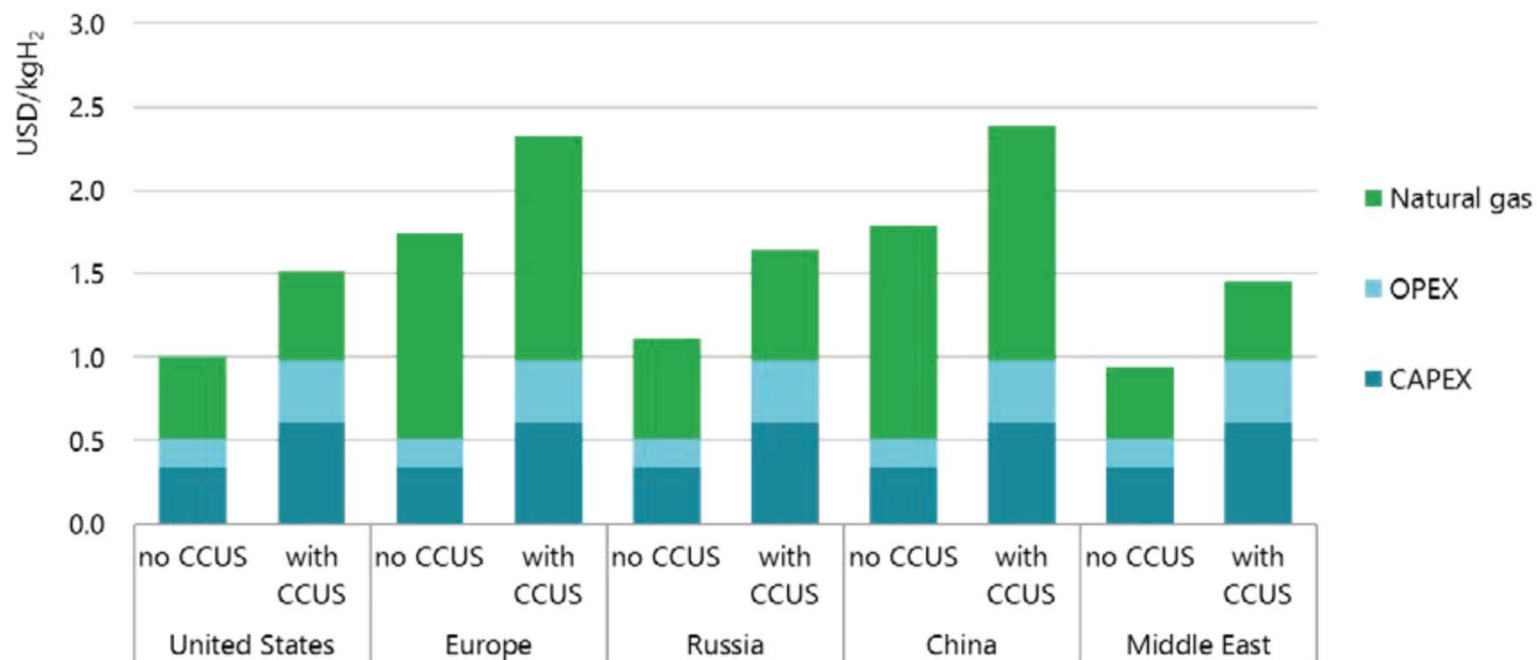


Notes: This map is without prejudice to the status of or sovereignty over any territory, to the delimitation of international frontiers and boundaries and to the name of any territory, city or area. Electrolyser CAPEX = USD 450/kWe, efficiency (LHV) = 74%; solar PV CAPEX and onshore wind CAPEX = between USD 400–1 000/kW and USD 900–2 500/kW depending on the region; discount rate = 8%.

Source: IEA analysis based on wind data from Rife et al. (2014), *NCAR Global Climate Four-Dimensional Data Assimilation (CFDDA) Hourly 40 km Reanalysis* and solar data from renewables.ninja (2019).

The Future of Hydrogen Report prepared by the IEA for the G20, Japan
Seizing today's opportunities., IEA June 2019

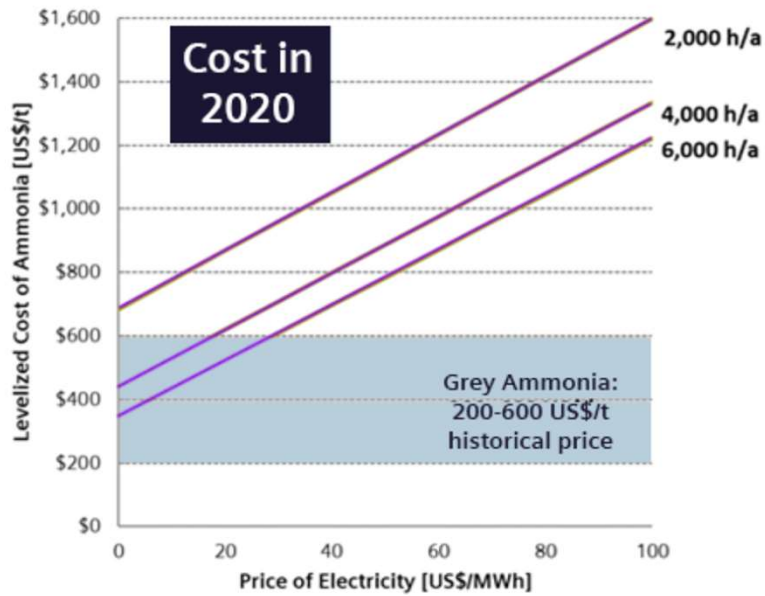
Hydrogen production costs using natural gas in different regions, 2018



Notes: kgH₂ = kilogram of hydrogen; OPEX = operational expenditure. CAPEX in 2018: SMR (steam methane reforming) without CCUS (carbon capture, utilisation and storage) = USD 500–900 per kilowatt hydrogen (kWh₂), SMR with CCUS = USD 900–1 600/kWh₂, with ranges due to regional differences. Gas price = USD 3–11 per million British thermal units (MBtu) depending on the region. More information on the underlying assumptions is available at www.iea.org/hydrogen2019.

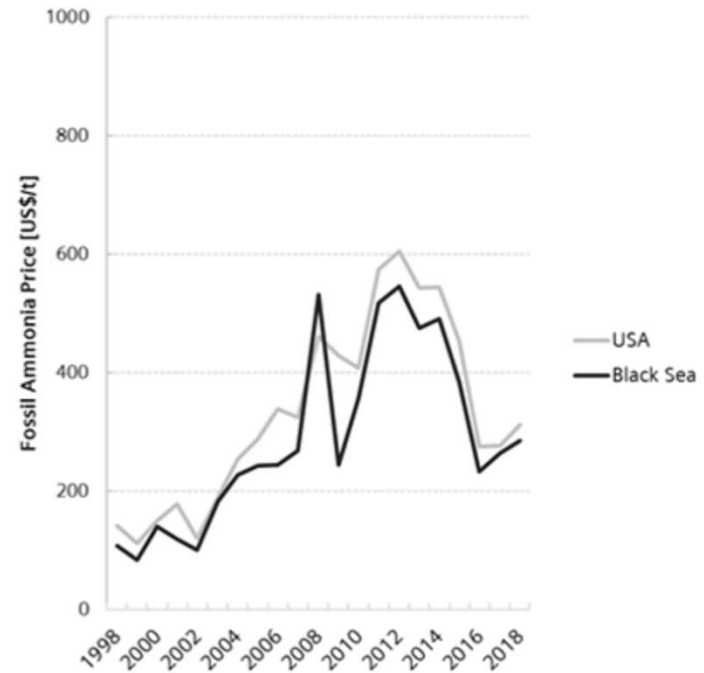
Source: IEA 2019.

e-ammonia's positive business case:
production cost is lower in geographies with
favourable renewable electricity resources



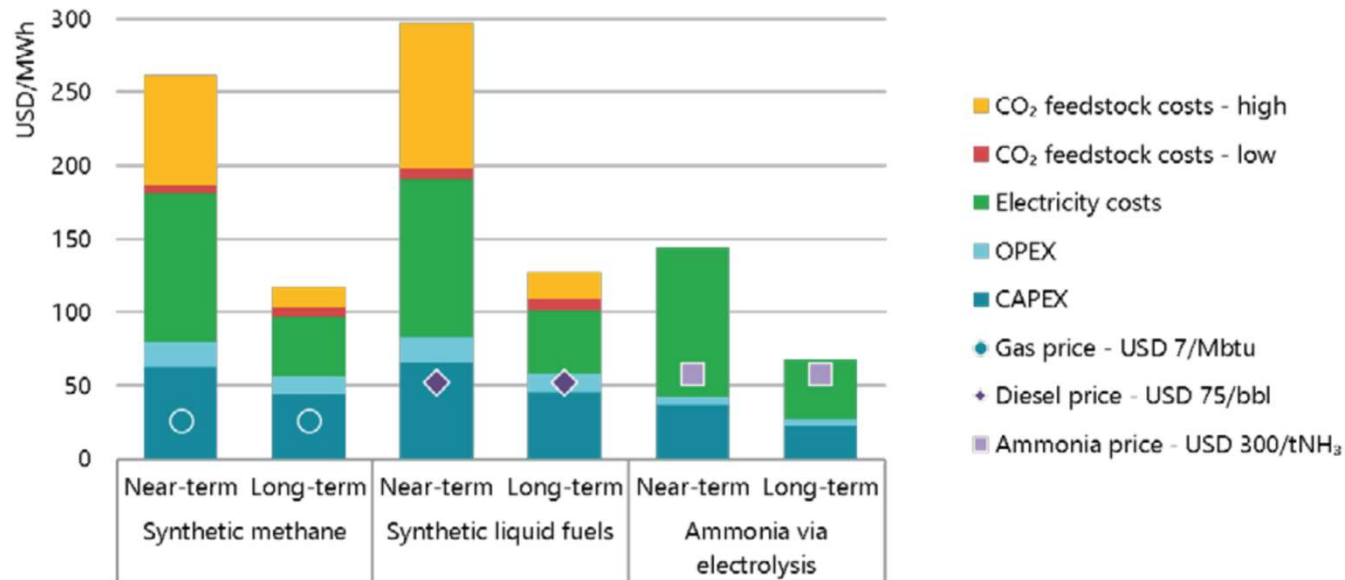
Source: Siemens. Assumptions: 2020 Prices. WACC 8%, Aboveground hydrogen storage (2 days) based on high HB flexibility.⁴ HB / ASU CAPEX based on 600 MTPD.³ No ammonia storage or transport considered.

Fossil fuel derived ammonia is subject to price
fluctuations and fossil fuel price volatility.



Source: Nutrien Factbook 2019

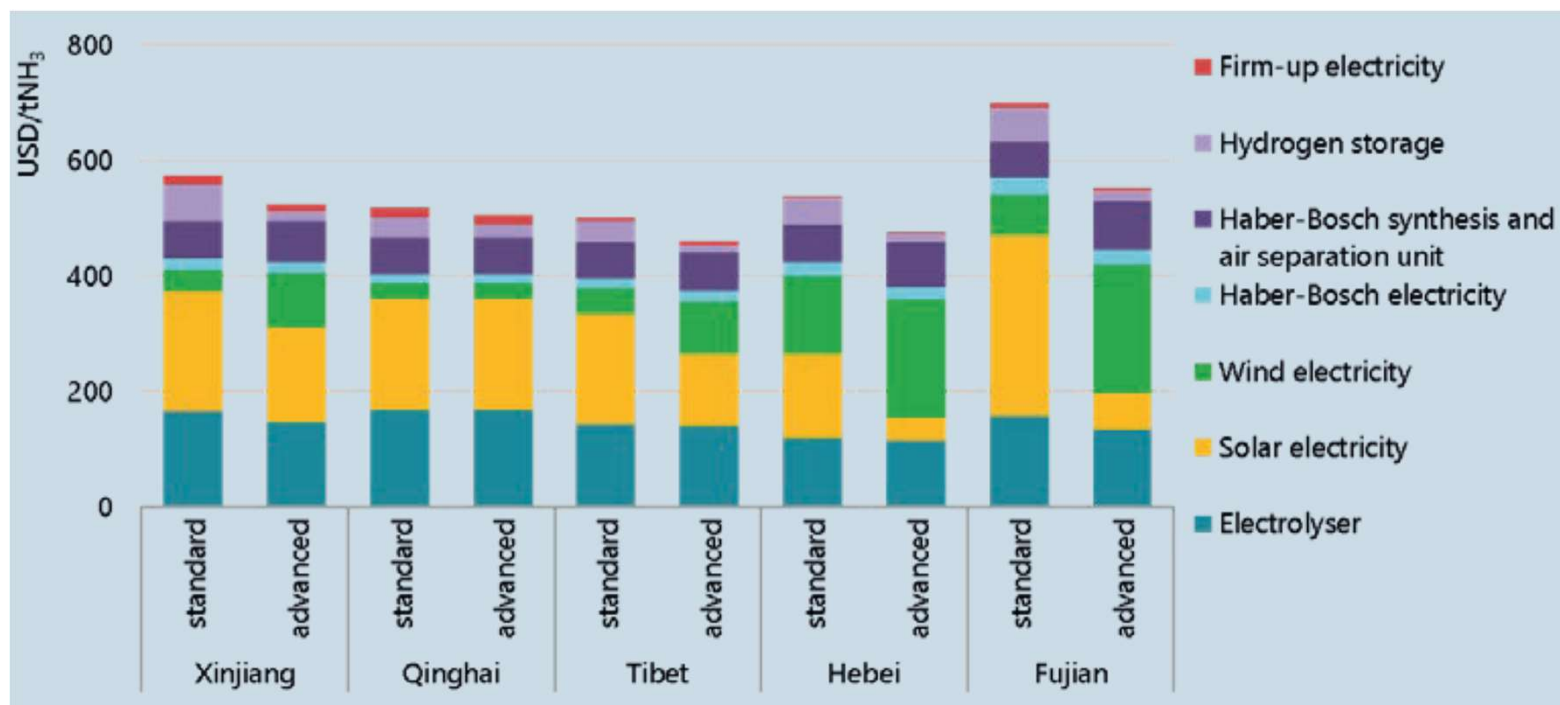
Indicative production costs of electricity-based pathways in the near and long term



Notes: NH₃ = ammonia.; renewable electricity price = USD 50/MWh at 3 000 full load hours in near term and USD 25/MWh in long term; CO₂ feedstock costs lower range based on CO₂ from bioethanol production at USD 30/tCO₂ in the near and long term; CO₂ feedstock costs upper range based on DAC = USD 400/tCO₂ in the near term and USD 100/tCO₂ in the long term; discount rate = 8%.

Source: IEA 2019.

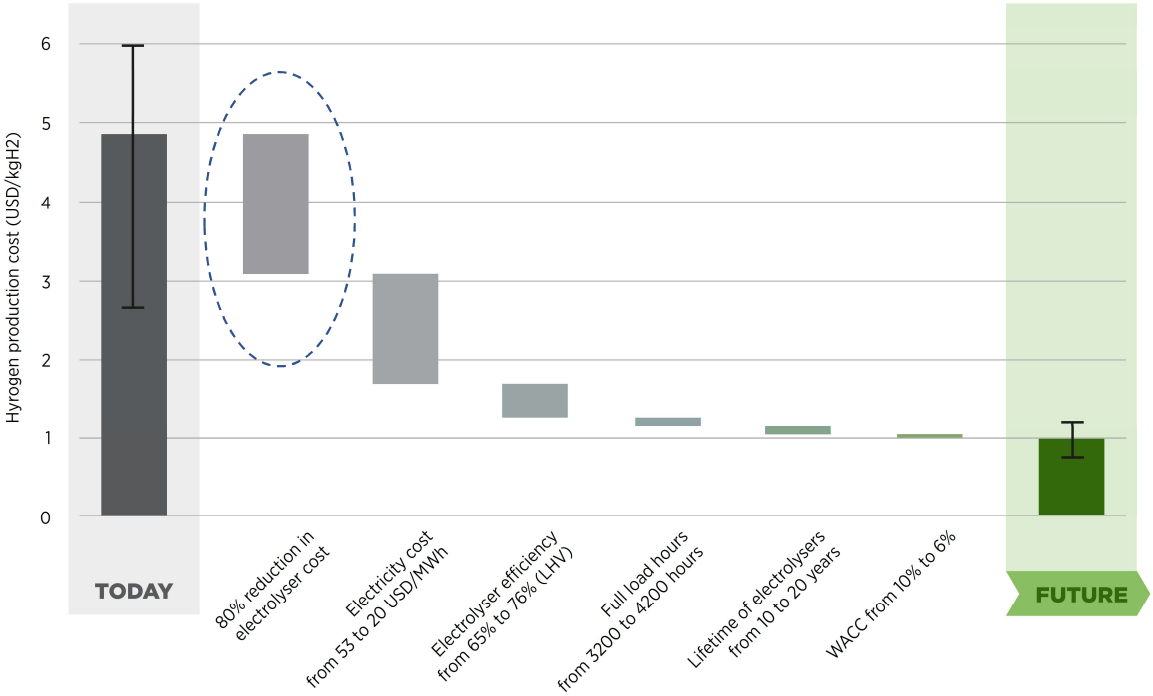
Estimated ammonia production costs from solar and wind in China, 2020



Notes: tNH₃ = tonne of ammonia. Left-hand bars correspond to “standard” flexibility of the Haber-Bosch operations with a 40% downward flexibility of the Haber-Bosch synthesis; right-hand bars correspond to the “advanced” flexibility case, allowing 80% downward flexibility and the possibility of shutting down the synthesis process completely. From bottom to top, the bars show the following costs: electrolyser, electricity from solar and wind for hydrogen production, renewable electricity for running the Haber-Bosch synthesis, Haber-Bosch synthesis and air separation unit for nitrogen production, hydrogen buffer storage and firm-up electricity to run the Haber-Bosch process when there is not enough wind at night.

Source: IEA 2019..

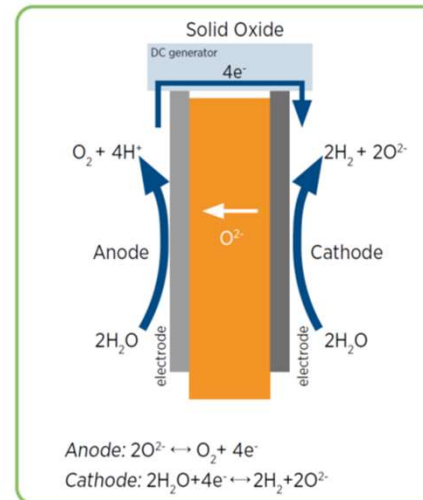
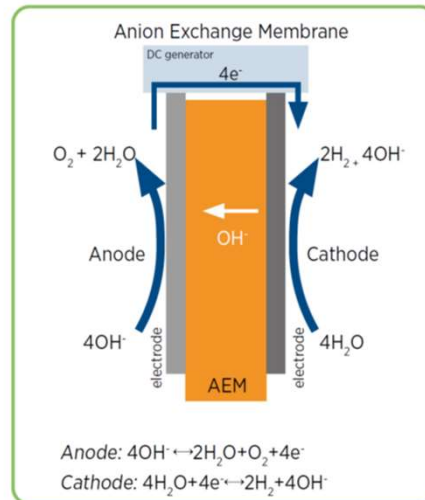
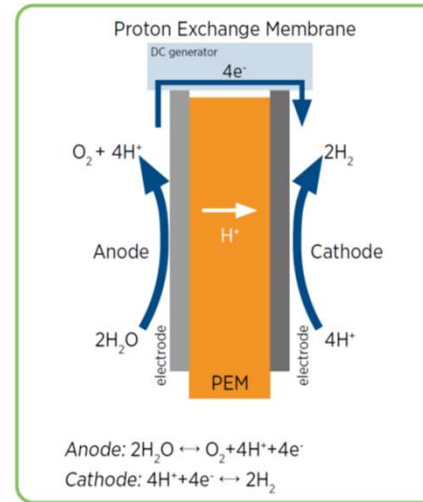
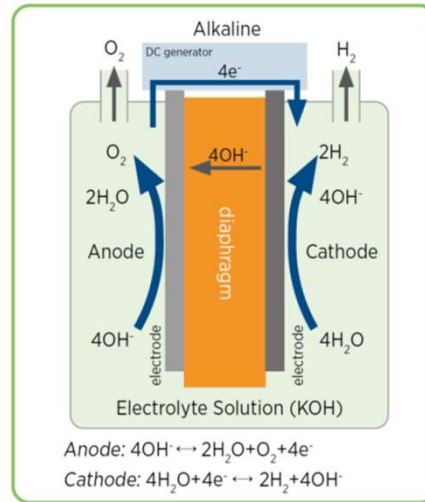
A combination of cost reductions in electricity and electrolyzers, combined with increased efficiency and operating lifetime, can deliver 80% reduction in hydrogen cost.



Note: ‘Today’ captures best and average conditions. ‘Average’ signifies an investment of USD 770/kilowatt (kW), efficiency of 65% (lower heating value – LHV), an electricity price of USD 53/MWh, full load hours of 3200 (onshore wind), and a weighted average cost of capital (WACC) of 10% (relatively high risk). ‘Best’ signifies investment of USD 130/kW, efficiency of 76% (LHV), electricity price of USD 20/MWh, full load hours of 4200 (onshore wind), and a WACC of 6% (similar to renewable electricity today).

Based on IRENA analysis (2020)

Different types of commercially available electrolysis technologies.



Based on IRENA analysis.

Characterisation of the four types of water electrolyzers.

	Alkaline	PEM	AEM	Solid Oxide
Operating temperature	70-90 °C	50-80 °C	40-60 °C	700-850 °C
Operating pressure	1-30 bar	< 70 bar	< 35 bar	1 bar
Electrolyte	Potassium hydroxide (KOH) 5-7 molL ⁻¹	PFSA membranes	DVB polymer support with KOH or NaHCO ₃ 1molL ⁻¹	Yttria-stabilized Zirconia (YSZ)
Separator	ZrO ₂ stabilized with PPS mesh	Solid electrolyte (above)	Solid electrolyte (above)	Solid electrolyte (above)
Electrode / catalyst (oxygen side)	Nickel coated perforated stainless steel	Iridium oxide	High surface area Nickel or NiFeCo alloys	Perovskite-type (e.g. LSCF, LSM)
Electrode / catalyst (hydrogen side)	Nickel coated perforated stainless steel	Platinum nanoparticles on carbon black	High surface area nickel	Ni/YSZ
Porous transport layer anode	Nickel mesh (not always present)	Platinum coated sintered porous titanium	Nickel foam	Coarse Nickel-mesh or foam
Porous transport layer cathode	Nickel mesh	Sintered porous titanium or carbon cloth	Nickel foam or carbon Cloth	None
Bipolar plate anode	Nickel-coated stainless steel	Platinum-coated titanium	Nickel-coated stainless steel	None
Bipolar plate cathode	Nickel-coated stainless steel	Gold-coated titanium	Nickel-coated Stainless steel	Cobalt-coated stainless steel
Frames and sealing	PSU, PTFE, EPDM	PTFE, PSU, ETFE	PTFE, Silicon	Ceramic glass

Note: Coloured cells represent conditions or components with significant variation among different companies. PFSA = Perfluoroacidsulfonic; PTFE = Polytetrafluoroethylene; ETFE = Ethylene Tetrafluoroethylene; PSF = poly (bisphenol-A sulfone); PSU = Polysulfone; YSZ = yttrastabilized zirconia; DVB = divinylbenzene; PPS = Polyphenylene sulphide; LSCF = $\text{La}_{0.58}\text{Sr}_{0.4}\text{Co}_{0.2}\text{Fe}_{0.8}\text{O}_{3-\delta}$; LSM = $(\text{La}_{1-x}\text{Sr}_x)\text{MnO}_3$; § = Crofer22APU with co-containing protective coating.

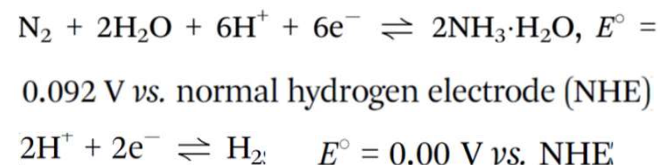
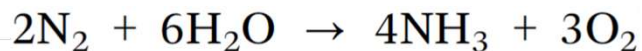
Based on IRENA analysis.

Key performance indicators for four electrolyser technologies today and in 2050.

	2020				2050			
	Alkaline	PEM	AEM	SOEC	Alkaline	PEM	AEM	SOEC
Cell pressure [bara]	< 30	< 70	< 35	< 10	> 70	> 70	> 70	> 20
Efficiency (system) [kWh/KgH ₂]	50-78	50-83	57-69	45-55	< 45	< 45	< 45	< 40
Lifetime [thousand hours]	60	50-80	> 5	< 20	100	100-120	100	80
Capital costs estimate for large stacks (stack-only, > 1 MW) [USD/kW _{el}]	270	400	-	> 2 000	< 100	< 100	< 100	< 200
Capital cost range estimate for the entire system, >10 MW [USD/kW _{el}]	500-1000	700-1400	-	-	< 200	< 200	< 200	< 300

Note: PEM = Polymer Electrolyte Membrane (commercial technology); AEM = Anion Exchange Membrane (lab-scale today); SOEC = Solid Oxide Electrolysers (lab-scale today).
Based on IRENA analysis.

Nitrogen Reduction Reaction (NRR)

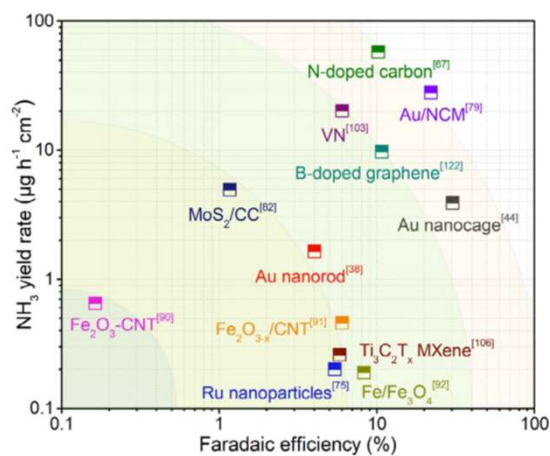
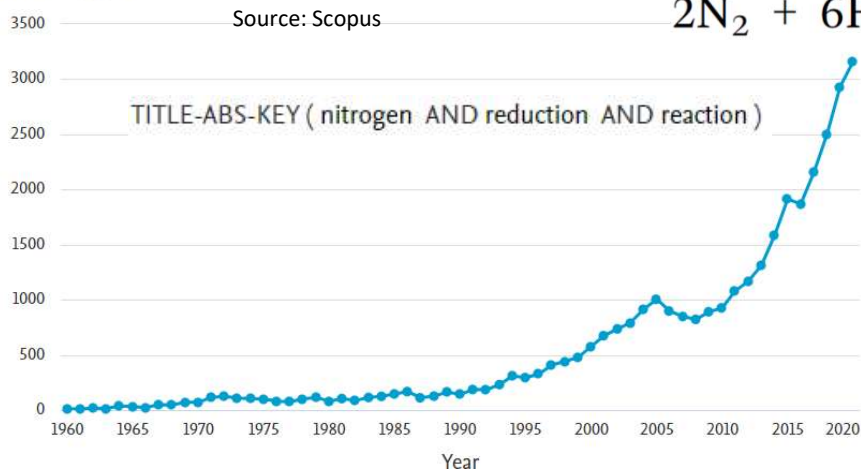


Documents by year

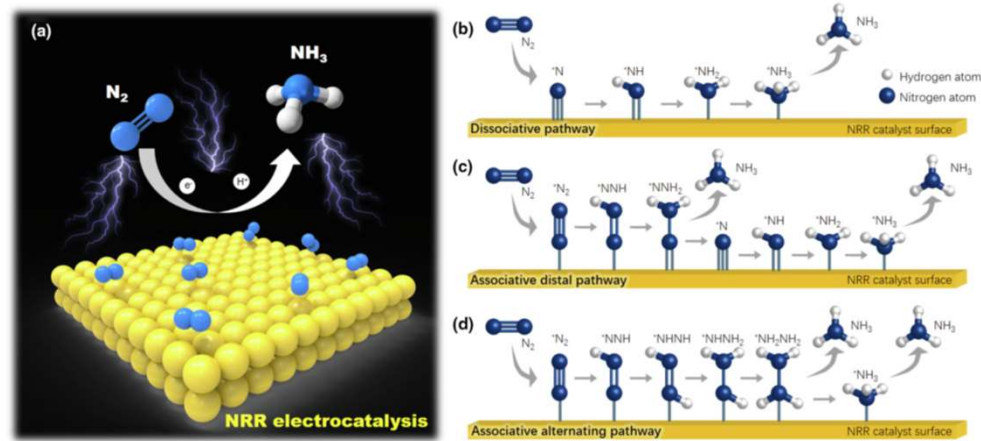
Source: Scopus

TITLE-ABS-KEY (nitrogen AND reduction AND reaction)

Documents

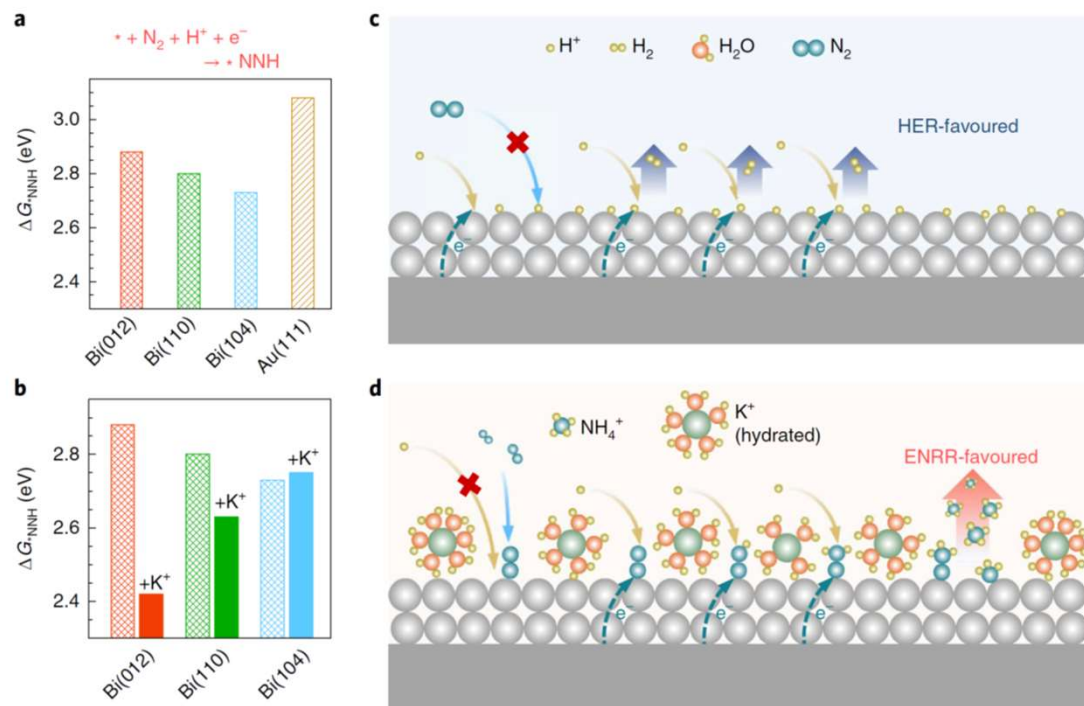


An NRR performance map of different catalysts in terms of the NH_3 yield rate and the Faradaic efficiency. (NCM: nitrogen-doped nanoporous carbonmembranes; CC: carbon cloth; CNT: carbon nanotube; $\text{Fe}_2\text{O}_{3-x}$: Fe_2O_3 -containing oxygen vacancies)



Schematic illustrations of (a) the nitrogen reduction reaction (NRR) electrocatalysis and its possible mechanisms, including (b) dissociative pathway, (c) associative distal pathway, and (d) associative alternating pathway

For electrochemical NH_3 synthesis to be competitive with the current H–B process, it would need to achieve at least a similar level of energy efficiency and NH_3 yield rate to the H–B process, i.e. $\sim 70\%$ and $\sim 30 \mu\text{mol h}^{-1} \text{mg}_{\text{cat}}^{-1}$, respectively. *Energy Environ. Sci.*, 2021, 14, 672687



Faradaic efficiency of 66% and ammonia yield of $200 \mu\text{mol mg}_{\text{cat}}^{-1} \text{h}^{-1}$

Hao, YC., Guo, Y., Chen, LW. *et al.* Promoting nitrogen electroreduction to ammonia with bismuth nanocrystals and potassium cations in water. *Nat Catal* 2, 448–456 (2019). <https://doi.org/10.1038/s41929-019-0241-7>

Promoting the NRR with bismuth catalysts and potassium cations.

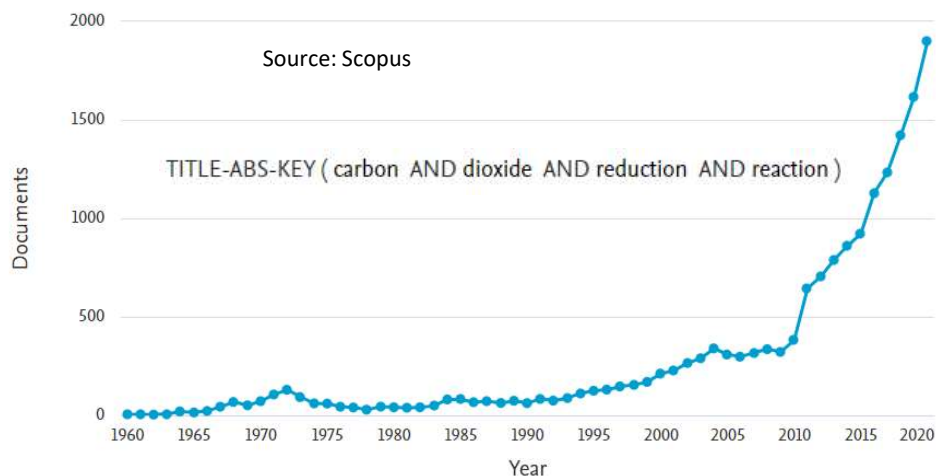
a, The free-energy change (ΔG^*_{NNH}) required to form $* \text{NNH}$ ($* + \text{N}_2 + \text{H}^+ + \text{e}^- \rightarrow * \text{NNH}$) on Bi (012), (110), (104) and Au (111) facets.

b, ΔG^*_{NNH} on Bi (012), (110) and (104) facets without (patterned bars) and with (filled bars) K^+ cations.

c,d, Mass transfer of protons and nitrogen molecules to the catalyst surface in electrolytes without (c) and with (d) K^+ cations. c, In acidic solutions without K^+ cations, protons can be transferred to the surface readily, and HER will dominate. d, K^+ hinders proton transfer to the catalyst surfaces. Nitrogen will be adsorbed preferentially, and the NRR is promoted.

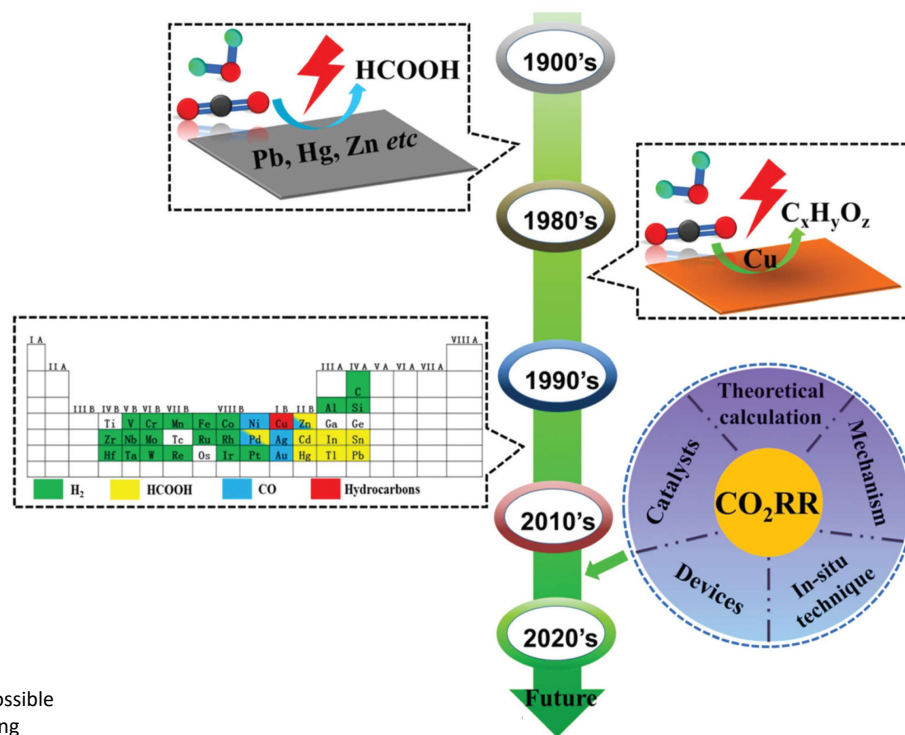
Carbon dioxide Reduction Reaction (CO₂RR)

Documents by year

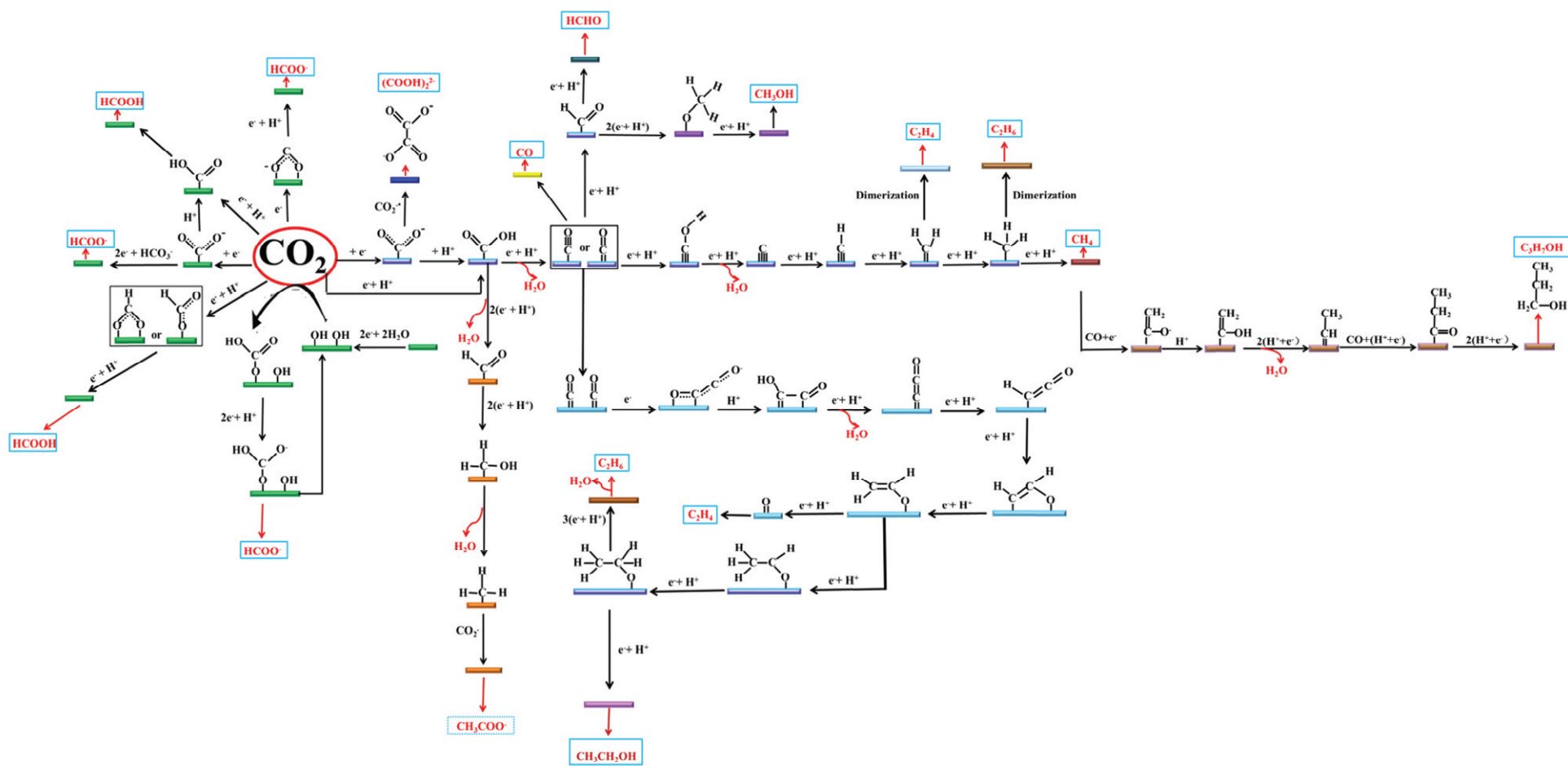


Reaction	E^0/V (vs. SHE)
$\text{CO}_2 + e^- \rightarrow \text{CO}_2^{\bullet-}$	1.90
$\text{CO}_2 + 2\text{H}^+ + 2e^- \rightarrow \text{CO} + \text{H}_2\text{O}$	-0.530
$\text{CO}_2 + 2\text{H}_2\text{O} + 2e^- \rightarrow \text{CO} + 2\text{OH}^-$	-1.347
$\text{CO}_2 + 2\text{H}^+ + 2e^- \rightarrow \text{HCOOH}$	-0.610
$\text{CO}_2 + \text{H}_2\text{O} + 2e^- \rightarrow \text{HCOO}^- + \text{OH}^-$	-1.491
$\text{CO}_2 + 4\text{H}^+ + 4e^- \rightarrow \text{HCHO} + \text{H}_2\text{O}$	-0.480
$\text{CO}_2 + 3\text{H}_2\text{O} + 4e^- \rightarrow \text{HCHO} + 4\text{OH}^-$	-1.311
$\text{CO}_2 + 6\text{H}^+ + 6e^- \rightarrow \text{CH}_3\text{OH} + \text{H}_2\text{O}$	-0.380
$\text{CO}_2 + 5\text{H}_2\text{O} + 6e^- \rightarrow \text{CH}_3\text{OH} + 6\text{OH}^-$	-1.225
$\text{CO}_2 + 8\text{H}^+ + 8e^- \rightarrow \text{CH}_4 + 2\text{H}_2\text{O}$	-0.240
$\text{CO}_2 + 6\text{H}_2\text{O} + 8e^- \rightarrow \text{CH}_4 + 8\text{OH}^-$	-1.072
$\text{CO}_2 + 4\text{H}^+ + 4e^- \rightarrow \text{C} + 2\text{H}_2\text{O}$	-0.200
$\text{CO}_2 + 2\text{H}_2\text{O} + 4e^- \rightarrow \text{C} + 4\text{OH}^-$	-1.040
$2\text{CO}_2 + 12\text{H}^+ + 12e^- \rightarrow \text{C}_2\text{H}_4 + 4\text{H}_2\text{O}$	-0.340
$2\text{CO}_2 + 8\text{H}_2\text{O} + 12e^- \rightarrow \text{C}_2\text{H}_4 + 12\text{OH}^-$	-1.177
$2\text{CO}_2 + 14\text{H}^+ + 14e^- \rightarrow \text{C}_2\text{H}_6 + 4\text{H}_2\text{O}$	-0.270
$2\text{CO}_2 + 2\text{H}^+ + 2e^- \rightarrow \text{H}_2\text{C}_2\text{O}_4$	-0.913
$2\text{CO}_2 + 2e^- \rightarrow \text{C}_2\text{O}_4^{2-}$	-1.003
$2\text{CO}_2 + 12\text{H}^+ + 12e^- \rightarrow \text{C}_2\text{H}_5\text{OH} + 3\text{H}_2\text{O}$	-0.330
$2\text{CO}_2 + 9\text{H}_2\text{O} + 12e^- \rightarrow \text{C}_2\text{H}_5\text{OH} + 12\text{OH}^-$	-1.157
$3\text{CO}_2 + 18\text{H}^+ + 18e^- \rightarrow \text{C}_3\text{H}_7\text{OH} + 5\text{H}_2\text{O}$	-0.320
$2\text{H}^+ + 2e^- \rightarrow \text{H}_2$	-0.420

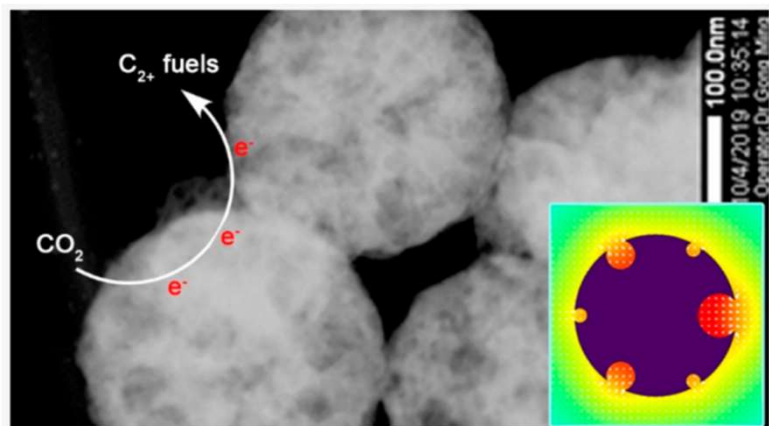
Half reactions of CO₂ reduction for possible processes along with the corresponding standard redox potential (25 °C, 1 atmosphere of gases and 1 M solutes in aqueous solution)



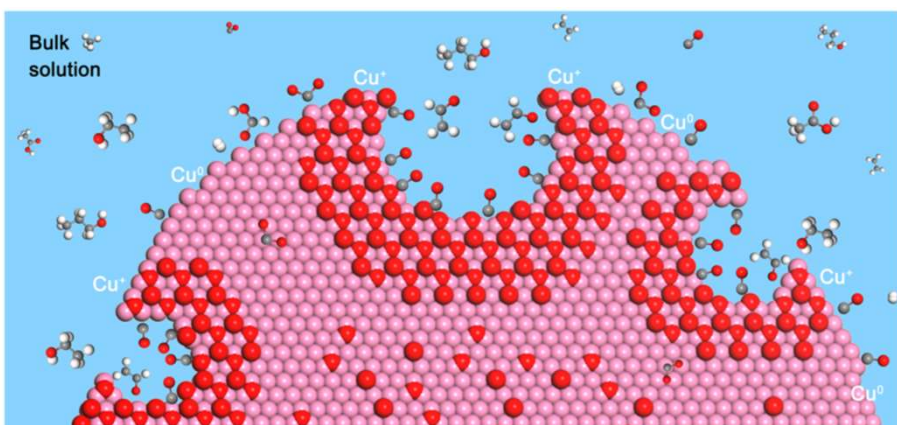
The possible reaction roadmap of CO₂



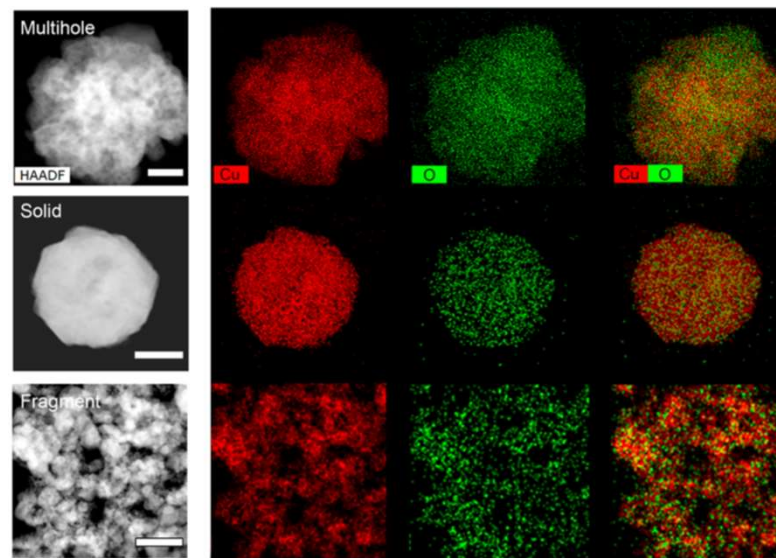
Continue improve in catalytic performances



Copper in the +1 oxidation state has been thought to be active for catalyzing C_{2+} formation, whereas it is prone to being reduced to Cu^0 at cathodic potentials. Catalysts with nanocavities can confine carbon intermediates formed in situ, which in turn covers the local catalyst surface and thereby stabilizes Cu^+ species. Experimental measurements on multihollow cuprous oxide catalyst exhibit a C_{2+} Faradaic efficiency of $75.2 \pm 2.7\%$ at a C_{2+} partial current density of $267 \pm 13 \text{ mA cm}^{-2}$ and a large C_{2+} -to- C_1 ratio of ~ 7.2 .



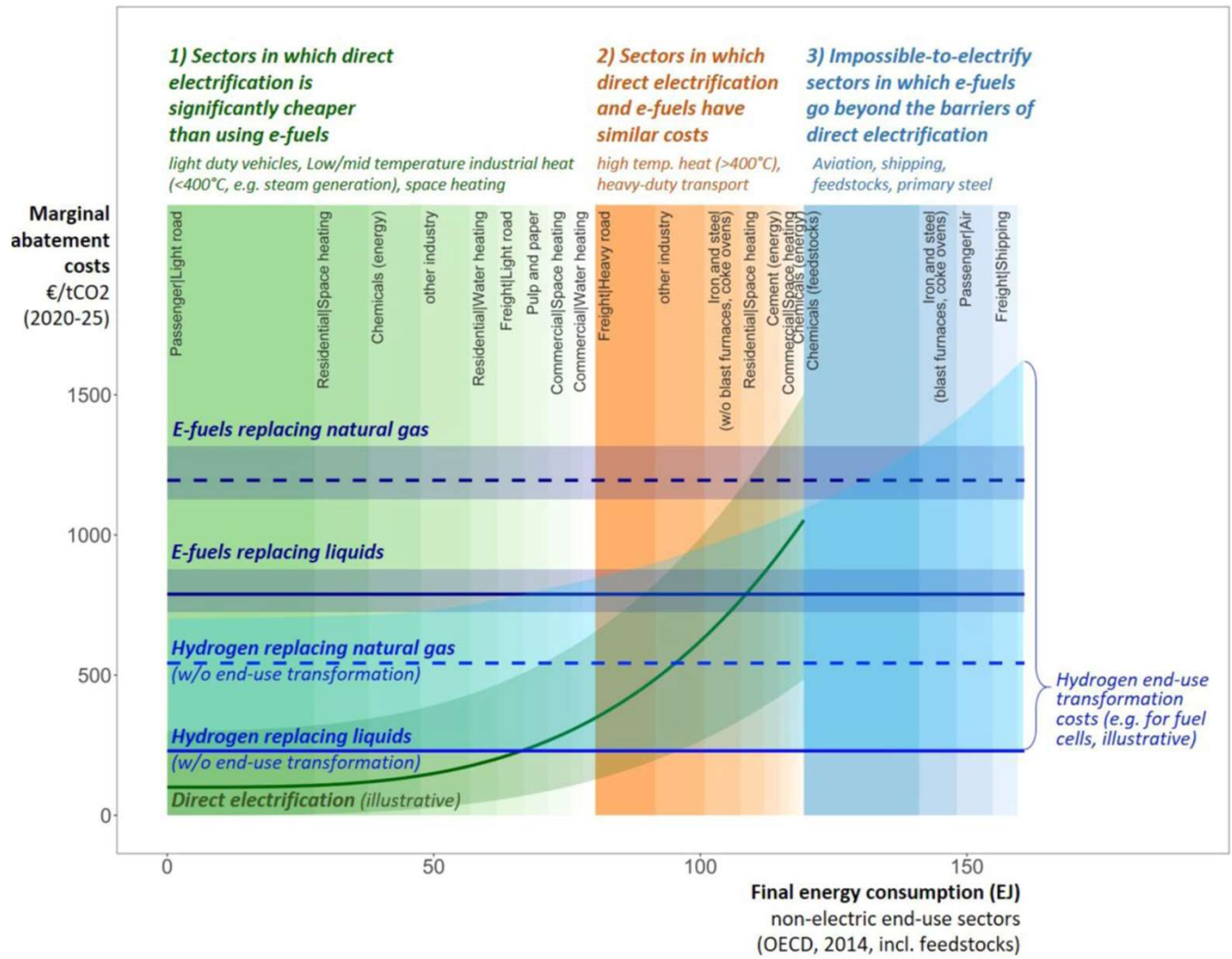
Schematic of carbon intermediates that are confined in the nanocavities, which locally protect copper oxidation state during CO_2RR . White: hydrogen; gray: carbon; red: oxygen; violet: copper.



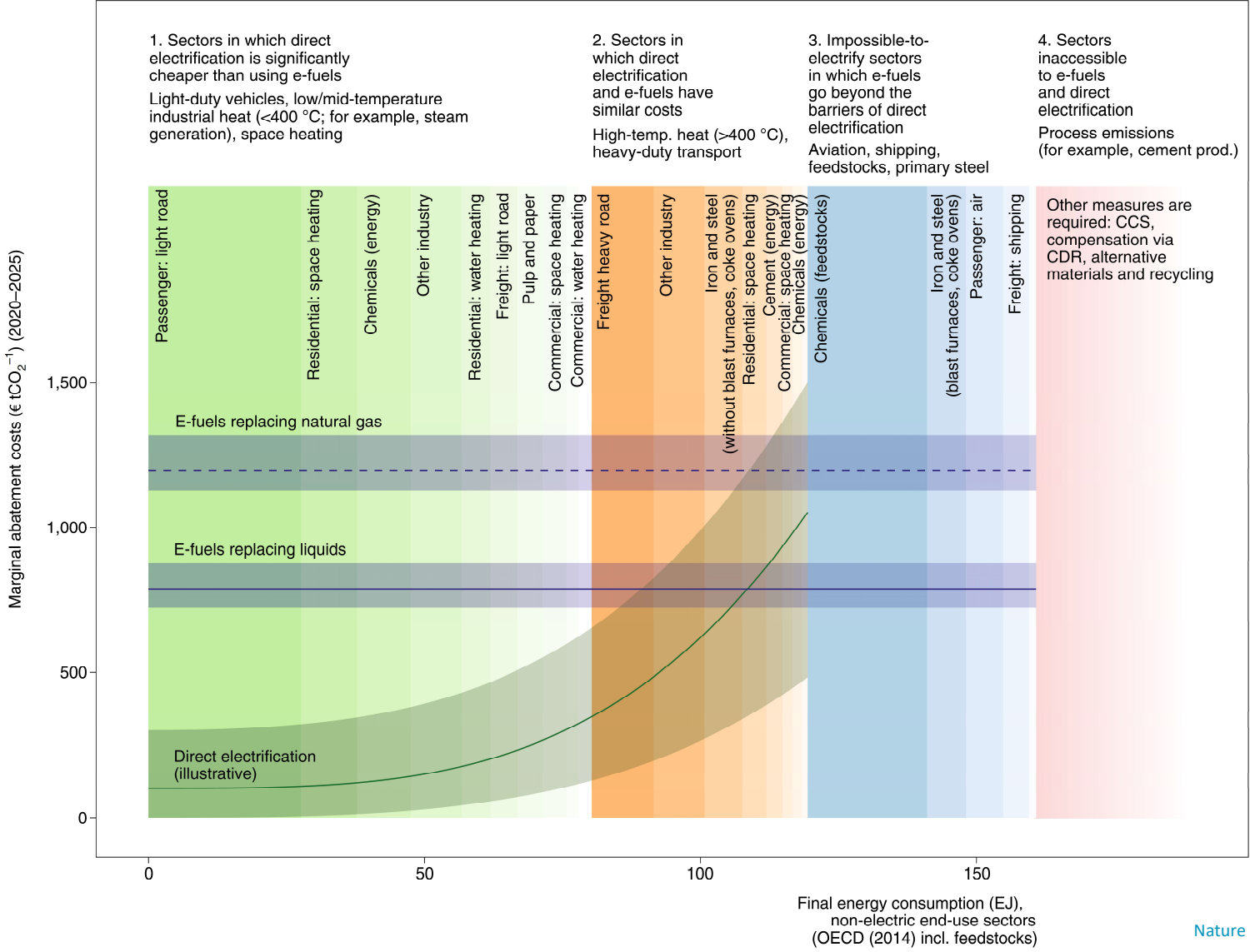
Scanning TEM-EDX elemental mapping of multihollow, solid, and fragment Cu_2O samples, showing the homogeneous distribution of Cu (red) and O (green).

J. Am. Chem. Soc. 2020, 142, 6400–6408

PERSPECTIVE



Marginal abatement cost curves including hydrogen (that is, fuel-switching CO₂ prices). In 2020–25 for e-methane (replacing natural gas), liquid e-fuels (replacing fossil liquids) and hydrogen (replacing liquids or gases) from the cost calculations as well as direct electrification alternatives (green, illustrative curve) across non-electric energy and industrial sectors in the OECD (2014 energy end-use data from IEA ETP 2017). The additional end-use transformation costs of using hydrogen are illustrative only. Shaded areas represent uncertainty ranges. The three categories of energy end uses are sorted according to the costs of directly electrifying the respective applications (horizontal sorting from low to high costs of direct electrification). Within each of the four categories, the sectors are sorted according to their size.



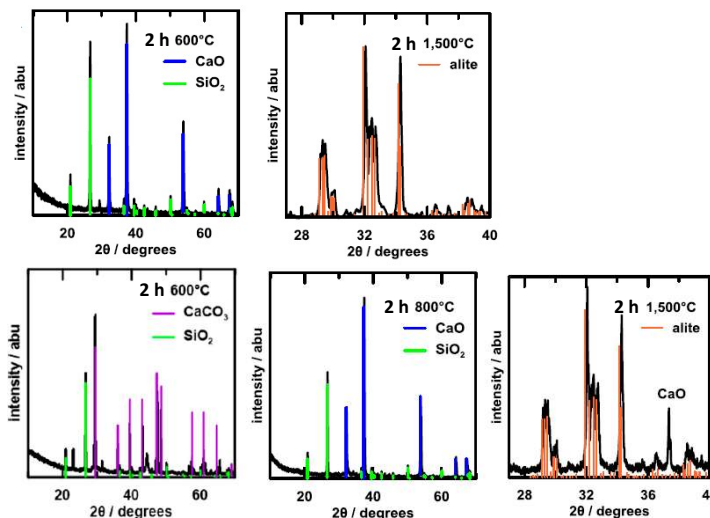
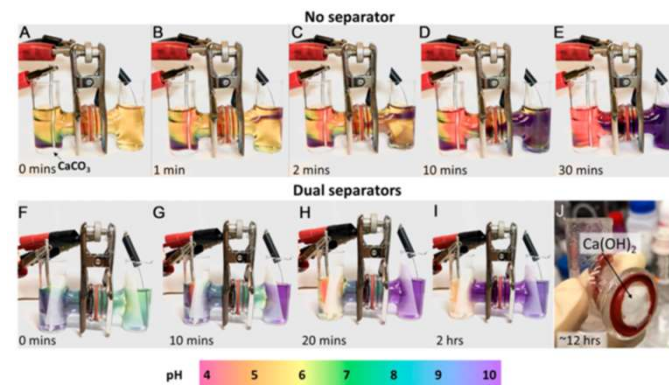
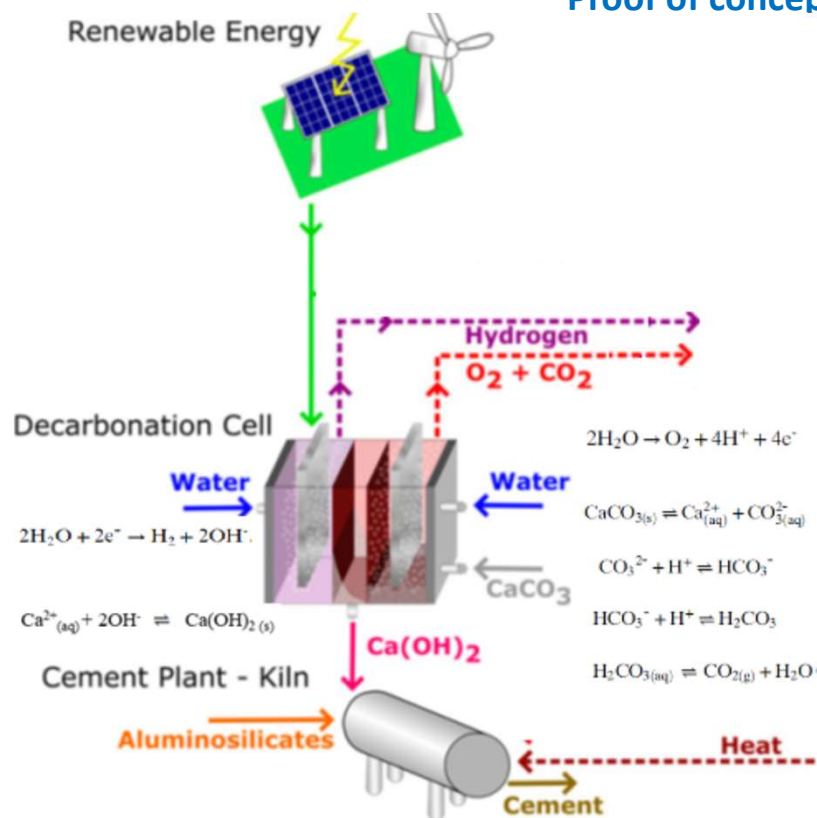
PERSPECTIVE

Marginal abatement cost curves (that is, fuel-switching CO₂ prices). Data in 2020–2025 for e-methane (replacing natural gas) and liquid e-fuels (replacing fossil liquids) from the cost calculations, and direct electrification alternatives (green, illustrative curve) across non-electric energy and industrial sectors in the OECD (2014 energy end-use data from IEA ETP 2017). The four categories of energy end uses are sorted according to the costs of directly electrifying the respective applications (horizontal sorting from low to high costs of direct electrification). Within each of the four categories, the sectors are sorted according to their size.

Electrochemical synthesis of cement

Cement production is currently the largest single industrial emitter of CO₂, accounting for ~8% (2.8 Gtons/y) of global CO₂ emissions. Deep decarbonization of cement manufacturing will require remediation of both the CO₂ emissions due to the decomposition of CaCO₃ to CaO and that due to combustion of fossil fuels (primarily coal) in calcining (~900 °C) and sintering (~1,450 °C).

Proof of concept



Conclusioni

- Le Tecnologie **Power to Chemicals** (ammoniaca e metanolo) sono vicine all'utilizzo con una forte driving force legata alla diminuzione dei costi dell'energia rinnovabile e dei costi di investimento degli elettrolizzatori.
- Nel settore dei carburanti l'approccio **e-fuel** non risulta competitivo rispetto all'utilizzo diretto dell'energia elettrica. Resta sicuramente da perseguire in questo settore l'utilizzo delle tecnologie waste to fuel.
- Le vie di sintesi **NRR** e **CO₂RR** sono arrivate in laboratorio a efficienze e produttività significative ma richiedono ancora forti investimenti in ricerca industriale.